

# Constraint on dark matter annihilation with dark star formation using Fermi extragalactic diffuse gamma-ray background data

Qiang Yuan<sup>a,b</sup>, Bin Yue<sup>c,d</sup>, Bing Zhang<sup>b</sup> and Xuelei Chen<sup>c,e</sup>

<sup>a</sup>*Key Laboratory of Particle Astrophysics, Institute of High Energy Physics, Chinese Academy of Sciences, Beijing 100049, P.R. China*

<sup>b</sup>*Department of Physics and Astronomy, University of Nevada Las Vegas, Las Vegas, NV 89154, USA*

<sup>c</sup>*National Astronomical Observatories, Chinese Academy of Sciences, Beijing 100012, P.R. China*

<sup>d</sup>*Graduate University of Chinese Academy of Sciences, Beijing 100049, P.R. China*

<sup>e</sup>*Center for High Energy Physics, Peking University, Beijing 100871, P.R. China*

*yuanq@mail.ihep.ac.cn, yuebin@bao.ac.cn, zhang@physics.unlv.edu,*

*xuelei@cosmology.bao.ac.cn*

**ABSTRACT:** It has been proposed that during the formation of the first generation stars there might be a “dark star” phase in which the power of the star comes from dark matter annihilation. The adiabatic contraction process to form the dark star would result in a highly concentrated density profile of the host halo at the same time, which may give enhanced indirect detection signals of dark matter. In this work we investigate the extragalactic  $\gamma$ -ray background from dark matter annihilation with such a dark star formation scenario, and employ the isotropic  $\gamma$ -ray data from Fermi-LAT to constrain the model parameters of dark matter. The results suffer from large uncertainties of both the formation rate of the first generation stars and the subsequent evolution effects of the host halos of the dark stars. We find, in the most optimistic case for  $\gamma$ -ray production via dark matter annihilation, the expected extragalactic  $\gamma$ -ray flux will be enhanced by 1 – 2 orders of magnitude. In such a case, the annihilation cross section of the supersymmetric dark matter can be constrained to the thermal production level, and the leptonic dark matter model which is proposed to explain the positron/electron excesses can be well excluded. Conversely, if the positron/electron excesses are of a dark matter annihilation origin, then the early Universe environment is such that no dark star can form.

**KEYWORDS:** dark matter annihilation, dark star, PopIII star formation, gamma rays.

---

## Contents

<b>1. Introduction</b>	<b>1</b>
<b>2. Formation rate of the first generation stars</b>	<b>2</b>
<b>3. EGRB from DM annihilation</b>	<b>5</b>
3.1 Enhancement factor of DM clumpiness	5
3.2 DM annihilation luminosity with DS formation	7
3.3 Gamma-ray flux and constraints on DM model parameters	8
<b>4. Conclusion and discussion</b>	<b>12</b>

---

## 1. Introduction

It has been proposed that there might be a new phase of the stellar evolution, dark (matter powered) star (DS), during the formation of the first generation stars (or Pop III stars) in the early time of the Universe (e.g., [1, 2, 3, 4, 5, 6, 7]). Collapse of the gas would attract dark matter (DM) to collapse together and form a high density core. Self-annihilation of DM particles would inject energy into the gas inside the core, which heats the gas core and prevents further collapse of the gas to initiate nuclear fusion. DSs typically have distinct features compared with normal stars [8], e.g., they are massive ( $500 - 1000 M_{\odot}$ ), large ( $1 - 10$  AU), and have low temperature ( $T_{\text{surf}} < 10000$  K). They might be detected with large telescopes [9, 10].

The impact of DS formation is very important in many aspects of astrophysics and cosmology. The reionization history of the Universe would be altered due to different contribution to the ionization photons from DSs [11]. The DS remnants might provide the seeds for super-massive black holes [1]. Moreover, the formation of DSs would result in a cuspier density profile of DM outside the stellar core<sup>1</sup>, which is expected to give an enhanced annihilation luminosity and can be reflected in the indirect detection signals such as  $\gamma$ -rays and neutrinos [11, 12].

In this work we aim to discuss the contribution of DM annihilation to the extragalactic  $\gamma$ -ray background (EGRB), within the framework of DS formation models. Schleicher et al. have studied the extragalactic background radiation for the DS scenario and derived the constraints on DM particle parameters [11]. There are several improvements or updates in the current study: 1) A more realistic prescription on the formation of Pop III stars

---

<sup>1</sup>Strictly speaking, it is the adiabatic contraction which results in a cuspier DM density profile, and due to the same reason a DS is formed. In the following when we say “DS enhancement” it actually means the enhancement induced by the contraction process to form DS.

(which can give birth to the DSs) is adopted; 2) The DM annihilation models are discussed extensively, especially for the leptonic DM models which may be responsible for the recent reported electron/positron excesses [13, 14, 15, 16, 17]; 3) The EGRB data is updated with the new result released by the Fermi team [18], which gives stronger constraints than the previous EGRET data [19].

Throughout the paper a flat  $\Lambda$ CDM cosmological model is adopted, and the cosmological parameters are adopted as the results of the combined analysis of the WMAP 5 year data and other cosmological measurements:  $\Omega_M = 0.274$ ,  $\Omega_\Lambda = 1 - \Omega_M$ ,  $\Omega_b = 0.046$ ,  $h = 0.705$ ,  $\sigma_8 = 0.812$ ,  $n_s = 0.96$  [20]. Adopting a different set of cosmological parameters does not alter the final results significantly. For example we have checked that the formation rate of first stars would change by less than several percent if we adopt the cosmological parameters derived with the WMAP 7 year data together with the baryon acoustic oscillation and  $H_0$  data [21].

This paper is organized as follows. In Sect. 2, we present the formation rate of first generation stars, which is tightly connected with the formation of DSs. In Sect. 3, we calculate the annihilation luminosity and  $\gamma$ -ray flux of both the scenarios with and without DS formation, and derive the constraints on DM model parameters. The conclusion and discussion are given in Sect. 4.

## 2. Formation rate of the first generation stars

We first introduce the mass function of the DM halos. The comoving number density distribution of DM halos can be expressed as

$$\frac{dn(z)}{dM} = \frac{\rho_X}{M} \sqrt{\frac{2A^2a^2}{\pi}} [1 + (av^2)^{-p}] \exp(-av^2/2) \frac{d\nu}{dM}, \quad (2.1)$$

where  $\nu = \delta_c(z)/\sigma(M)$ ,  $\delta_c(z) = 1.68/D(z)$  is the critical over-density in spherical collapse model,  $D(z)$  is the linear growth factor [22].  $A$ ,  $a$  and  $p$  are constants. For  $(A, a, p) = (0.5, 1, 0)$  it is the Press-Schechter (PS) formula [23], and for  $(A, a, p) = (0.322, 0.707, 0.3)$  it is Sheth-Tormen (ST) formula [24]. In this work we adopt the ST mass function.  $\sigma^2(M)$  is the average variance of density field

$$\sigma^2(M) = \frac{1}{2\pi^2} \int W^2(kR_M) P_\delta(k) k^2 dk, \quad (2.2)$$

with the top-hat window function  $W(x) = 3(\sin x - x \cos x)/x^3$ .  $R_M = (3M/4\pi\rho_m)^{1/3}$  is a radius within which a mass  $M$  is contained with a uniform matter density field. The matter power spectrum  $P_\delta(k)$  is expressed as

$$P_\delta(k) = A_s(k \cdot \text{Mpc})^{n_s} T^2(k), \quad (2.3)$$

where  $A_s$  is normalized using  $\sigma_8$ , transfer function  $T(k)$  is obtained from a fit of  $\Lambda$ CDM model [25],

$$T(q) = \frac{\ln(1 + 2.34q)}{2.34q} [1 + 3.89q + (16.1q)^2 + (5.46q)^3 + (6.71q)^4]^{-0.25} \quad (2.4)$$

with  $q = k/h\Gamma$  and  $\Gamma = \Omega_m h \exp[-\Omega_b(1 + \sqrt{2h}/\Omega_m)]$ .

In the early Universe, the first stars would form in halos that are massive enough for gas to cool and condense. The number of such halos increases rapidly, and the halo destruction by mergers can be neglected. We therefore assume that the Star Formation Rate (SFR) of the first generation stars is proportional to the redshift derivative of the halo mass function  $\frac{d^2n}{dMdz}$  within a certain mass range [26], with a time delay  $\tau_d$  due to the cooling and collapse of the halo [27]. At a given redshift  $z$ , the SFR can be written as

$$\text{SFR}_{\text{PopIII}}(z) = \int_z^\infty \int_{M_{\min}(z'')}^{M_{\max}(z'')} \left| \frac{d^2n}{dMdz} (M, z'') \right| [1 - Q_{\text{H}^+}(z'')] \delta[z - z'(\tau_d, z'')] dM' dz'', \quad (2.5)$$

where  $Q_{\text{H}^+}$  is the volume-filling factor of  $\text{H}^+$  regions,  $z'(\tau_d, z'')$  is the redshift with time  $\tau_d$  delay of  $z''$ . Here we further assume that only one first generation star could form in each potential halo<sup>2</sup>. The  $\delta$  function in Eq. (2.5) means that the halos which satisfy the formation condition of the first stars will eventually contribute to the SFR  $\tau_d$  later. For the time delay, we adopt  $\tau_d = \tau_{\text{cool}} + \tau_{\text{ff}}$ , in which the cooling time scale for  $\text{H}_2$  is  $\tau_{\text{cool}} = 2.38 \times 10^{13} \left( \frac{M}{10^6 M_\odot} \right)^{-2.627} \left( \frac{1+z}{31} \right)^{-6.94}$  s and the free fall time scale is  $\tau_{\text{ff}} = 2.77 \times 10^{14} \left( \frac{1+z}{31} \right)^{-3/2}$  s [27]. This delay time scale  $\tau_d$  is mass-dependent, which makes the calculation of Eq. (2.5) more complicated.

As for the lower mass limit, it is usually believed that the first generation stars could only form in halos with virial temperature above  $10^3$  K if the coolant is  $\text{H}_2$ . However, in the presence of Lyman-Werner (LW) photons which are emitted by stars which form previously, this lower limit increases since only  $\text{H}_2$  in massive enough halos can survive from the photo-dissociation. Following Ref. [27], the lower limit of the halo mass  $M_{\min}$  for the first star formation would be the maximum of  $M_{\text{H}_2-\text{cool}} = 6.44 \times 10^6 M_\odot J_{21}^{0.457} \left( \frac{1+z}{31} \right)^{-3.557}$  and  $M_{\text{vir}}(10^3 K, z)$ , with  $J_{21}$  the specific intensity of LW radiation in unit of  $10^{-21}$  erg  $\text{s}^{-1} \text{cm}^{-2} \text{Hz}^{-1} \text{sr}^{-1}$ .

The upper limit can be adopted as the virial mass corresponding to a virial temperature of  $10^4$  K. It is generally believed that within halos with  $T_{\text{vir}} > 10^4$  K, the cooling by atomic Hydrogen excitation becomes more efficient, so that the gas would fragment into multiple parts and the massive and isolated first generation stars cannot form.

The intensity of LW radiation from the first generation stars is

$$J_{\text{LW}}^{\text{PopIII}}(z) = 4\pi \int_z^{z_s} n_{\text{PopIII}}(z') (1+z')^2 \epsilon_{\text{LW}} \frac{dl}{dz'} dz', \quad (2.6)$$

in which  $\epsilon_{\text{LW}}$  is the emissivity of LW photons,  $\frac{dl}{dz'}$  is the comoving distance per redshift,  $z_s$  is the upper limit above which the LW photons would be redshifted out of this band, i.e.  $z_s = 13.6/11.2(1+z) - 1$ .  $n_{\text{PopIII}}(z)$  is the comoving number density of active first generation stars, which can be obtained through integrating SFR with respect to redshift within the life time of such stars

$$n_{\text{PopIII}}(z) = \int_{z+\Delta z(\tau_{\text{PopIII}})}^z \text{SFR}_{\text{PopIII}}(z') dz'. \quad (2.7)$$

---

<sup>2</sup>There has been no discussion on whether DSs can form if fragmentation is important during first star formation (e.g., [28]). Our discussion does not apply to those scenarios.

We adopt a typical mass of  $200 M_{\odot}$  of the first stars in this work. According to Ref. [29], the life time of such a star is  $\simeq 2.24$  million years, and  $\epsilon_{\text{LW}} \simeq 1.15 \times 10^{25} \text{ erg s}^{-1} \text{ Hz}^{-1}$ . The choice of this mass is consistent with the numerical simulations of first stars. If the mass parameter alters by a factor of several, the main influence would be the LW feedback. As discussed below, we will investigate the LW feedback efficiency within a wide range. This effectively includes the variance of the first star mass to some extent. We also note that if the initial mass function (IMF) of the first stars follows a Salpeter form between  $100 M_{\odot}$  and  $500 M_{\odot}$  [30], the LW emission rate per unit star mass is close to that of a  $200 M_{\odot}$  star.

Note that DS formation may also affect the LW feedback. First, DSs will also produce LW photons. However, for typical DS parameters,  $L \sim 10^6 - 10^7 M_{\odot}$ ,  $T \sim 5000 - 10000 \text{ K}$  [8], we find that the contribution to LW emissivity ( $11.2 - 13.6 \text{ eV}$ ) is negligible. Second, after the DS stage, the object will enter the main sequence as a traditional star powered by nuclear fusion, with different properties from the ordinary PopIII star. There is no clear conclusion about the properties and fate of this particular main sequence star (e.g., [8, 9, 31, 32]). In any case, since we have employed a large range of uncertainty of LW feedback (see below), the impact of DS formation on the first star formation rate would not introduce much larger uncertainties, and we have neglected this effect in the following discussion.

Besides the first generation stars, there are also galaxies that can contribute to the LW dissociation and ionization process. SFR of metal-enriched and metal-free galaxies are:

$$\text{SFR}_{\text{gal}}^{\text{en}} = p_{\text{en}}(z) \times \frac{\Omega_b}{\Omega_m} f_{\star} \int_{M_{\text{vir}}(10^4 \text{K}, z)}^{\infty} \frac{d^2 n}{dM dz}(M, z) dM \quad (2.8)$$

and

$$\text{SFR}_{\text{gal}}^{\text{fr}} = [1 - p_{\text{en}}(z)] \times \frac{\Omega_b}{\Omega_m} f_{\star} \int_{M_{\text{vir}}(10^4 \text{K}, z)}^{\infty} \frac{d^2 n}{dM dz}(M, z) dM \quad (2.9)$$

respectively, where  $f_{\star} = 2 \times 10^{-3}$  is the fraction of gas that converts to stars, and  $p_{\text{en}}$  is the enrichment probability of gas by metals. The enrichment probability could be divided into two parts: the self-enrichment through which a Pop III star could pollute the host halo, and the probability that a halo is polluted by metals from neighbors. We follow Ref. [33] to calculate the self-enrichment probability. The pollution probability from neighbors is assumed to be just the metal fraction of the Universe. According to Ref. [34], almost one half of the mass of a Pop III star would be released through pair instability supernova (PISN), and the metal yield from galaxies is about 0.04 [35]. As for the LW photons emitted by galaxies, we take a time-evolved emissivity from Ref. [36], and add this part to Eq. (2.6).

We also trace the reionization evolution history, since it could reduce the SFR of first generation stars by a factor  $1 - Q_{\text{H}+}$ . The evolution of  $Q_{\text{H}+}$  is described as [11]

$$\frac{dQ_{\text{H}+}}{dz} = \frac{Q_{\text{H}+} C(z) n_{\text{H}+} \alpha_A}{H(z)(1+z)} + \frac{dn_{\text{ph}}/dz}{n_{\text{H}}}, \quad (2.10)$$

where  $C(z) = 27.466 \exp(-0.114z + 0.001328z^2)$  is the clumping factor [37],  $n_{\text{H}+}$  is the number density of ionized hydrogen,  $\alpha_A$  is the recombination coefficient [38],  $H(z)$  is the

Hubble parameter, and  $n_{\text{H}}$  is the mean neutral hydrogen density. In our work, the production of ionization photons  $dn_{\text{ph}}/dz$  is expressed as

$$\frac{dn_{\text{ph}}}{dz}(z) = (1+z)^3 \left[ n_{\text{PopIII}}(z)\epsilon_{\text{ph}} + \int_{\infty}^z \text{SFR}_{\text{gal}}(z')\epsilon_{\text{gal}}(z-z')dz' \right] \frac{dt}{dz}. \quad (2.11)$$

The first term refers to the contribution from first generation stars. For a  $200 M_{\odot}$  metal-free star the emissivity of ionization photons  $\epsilon_{\text{ph}}$  is  $3.1 \times 10^{50} \text{ s}^{-1}$  [29]. The second term is the contribution from the galaxies, including metal-enriched and metal-free galaxies. In the second term,  $\epsilon_{\text{gal}}$  is a time-evolved emissivity of ionization photons, which is adopted from Ref. [36].

There are still large uncertainties about the LW feedback mechanism due to the lack of understanding of the self-shielding [39]. Furthermore, the molecular hydrogen in the relic HII regions may also absorb some LW photons, reducing the effect of photo-dissociation. To consider such a reduction on the LW intensity, we employ a free parameter  $f_{\text{LW}}$  to represent the efficiency of LW feedback.

Combining Eqs. (2.5)–(2.11) together, we can get a coupled equation set of the SFR at a given redshift. This equation set depends on the evolution history of SFR, so it should be integrated step by step from an initial time. At a high redshift, e.g. around 60,  $J_{\text{LW}}$  is negligible, SFR could be obtained directly by setting  $M_{\text{min}} = M_{\text{vir}}(10^3 \text{ K}, z)$ . With this initial value, the SFR at first step after the initial redshift could be calculated by the set of equations discussed above. Performing the same calculation step by step, we can finally obtain the entire evolution history of the SFR.

The SFRs of Pop III stars for different LW efficiencies  $f_{\text{LW}} = 0.0, 10^{-4}, 10^{-2}$ , and 1.0 are shown in Fig. 1. It is shown that for the very effective LW feedback the star formation ends very early, at  $z \sim 25$ . For the most optimistic case without LW feedback the star formation can last till  $z \sim 6$ . These two extreme cases may represent the lower and upper limits of the SFR of the first generation stars.

### 3. EGRB from DM annihilation

#### 3.1 Enhancement factor of DM clumpiness

In this section we describe the enhancement factor of DM annihilation due to clumpiness, defined as the ratio between DM annihilation rate with structures and that of smoothly distributed case. We first consider the standard case without DS formation. The details of the calculation of the enhancement factor of the extragalactic DM annihilation can be referred to Refs. [41, 42]. Here we quote the basic formulae. The density profile of all the halos is assumed to be NFW profile [43]

$$\rho(r) = \frac{\rho_s}{(r/r_s)(1+r/r_s)^2} \quad (3.1)$$

with two scale parameters  $r_s$  and  $\rho_s$ . The scale radius  $r_s$  is determined by the concentration parameter  $c_v$  of the halo

$$r_s = r_v/c_v, \quad (3.2)$$

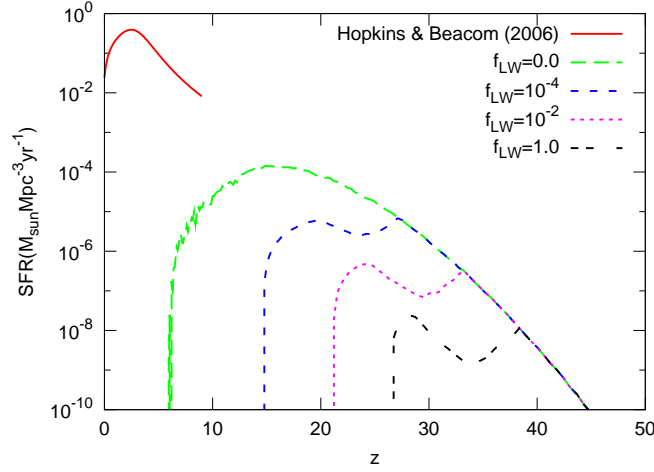


**Figure 1:** The evolution of SFR of first generation stars. In this plot the SFR is the result of Eq. (2.5) multiplied by  $M_{\text{fs}} dz/dt$  to convert to the usual definition. The solid curve is the fit to the observational SFR for the second and third generation stars [40].

where  $r_v$  is the virial radius. The scale density  $\rho_s$  is then determined by normalizing the mass of the halo to  $M$ . Note that there is no consensus about the density profile at the innermost part of the halo [44, 45, 46, 47, 48]. For different density profiles of the halos, the annihilation signals would differ from each other very much. However, as shown in [1], the density profiles of the DM halo after adiabatic contraction are very similar to each other even for very distinct initial density profiles. Since in this work we mainly focus on the effects of the adiabatic contraction (DS formation), we do not discuss in detail the effect of different halo density profiles.

The concentration parameter as a function of halo mass  $M$  can be extracted from N-body simulations. For the low mass halos which are beyond the resolution of simulations, the concentration is obtained by extrapolation. In this paper we consider two concentration models. One is the semi-analytical model developed in Ref. [49] with the update of WMAP5 cosmological parameters, which is labeled as “B01”. The other model is to extrapolate the power-law fitting results from the numerical simulations based on the WMAP5 cosmological parameters [50] directly to the low mass range, which is labeled as “power-law”. For both models we employ the redshift evolution  $c_v(z) = c_v(z=0)/(1+z)$  [49]. The results of B01 and power-law models do not differ very much from each other at high mass scales ( $M \gtrsim 10^5 M_\odot$ ). However, when extrapolating to lower mass scales, power-law concentration would be larger than B01 model, and hence gives larger annihilation signals. The halos which can give birth to DSs are massive enough that the DS enhancement between these two concentration models will be very similar. There are some updated concentration models which show different mass-dependence and redshift evolution (e.g., [51, 52]), however, they will also suffer from the uncertainties when extrapolating to low mass halos.

The total annihilation luminosity for a population of DM halos with comoving number

density distribution  $dn(z)/dM$  is given as

$$L_{\text{tot}}(z) = \int dM \frac{dn(z)}{dM} (1+z)^3 L(M, z), \quad (3.3)$$

where  $(1+z)^3$  is to convert the comoving halo mass function to the physical one, and  $L(M, z) = 4\pi \int_0^{r_v} \rho^2(r) r^2 dr$  is the annihilation luminosity of a single halo. For the mass function  $dn(z)/dM$  please refer to the Appendix. The enhancement factor is then

$$\Delta^2(z) \equiv \frac{L_{\text{tot}}}{\rho_\chi^2 (1+z)^6}, \quad (3.4)$$

where  $\rho_\chi$  is the average DM density of the Universe today.

### 3.2 DM annihilation luminosity with DS formation

If there is DS formation following the first generation stars, the annihilation luminosity will be enhanced. The annihilation luminosity of the halos which ever contained DSs can be calculated as

$$\begin{aligned} L_{\text{tot}}^{\text{ds}}(z) &= (1+z)^3 \int_{z+\Delta z(\tau_{\text{ds}})}^z dz' \\ &\times \int_{z'}^\infty \int_{M_{\text{min}}(z''')}^{M_{\text{max}}(z''')} f_{\text{ds}} L(M, z''') [1 - Q_{\text{H}^+}(z''')] \frac{d^2 n}{dM dz'} (M, z''') \\ &\times \delta[z' - z''(\tau_d, z''')] dM dz''', \end{aligned} \quad (3.5)$$

where  $f_{\text{ds}}$  is the enhancement factor of the annihilation luminosity of a single halo after DS formation compared with the original density profile, and  $\tau_{\text{ds}}$  is the age of the halo which hosts a DS. Generally speaking the density profile would steepen as  $r^{-1.9}$ , regardless of the initial density profile of the DM halo. We note, however, that the detailed density profile would depend on the parameters of the initial DM halo and the collapsing gas core. According to the density profile of halos after DS formation [53], we estimate  $f_{\text{ds}} \sim 10^3$  compared with initial NFW profile. Such a value is consistent with that estimated in [11].

If there is only an annihilation effect to consume the DM,  $\tau_{\text{ds}}$  is estimated to be much longer than the age of the Universe, and the lower limit of the redshift integral ( $dz'$ ) can be taken as  $\infty$ . On the other hand, in order to qualitatively take into account the evolution effect of the halos after the DS formation, we also take another conservative approach by considering that the halo with DS formation can only exist for a finite time due to possible mergers with other halos<sup>3</sup>. Following Ref. [33], for a halo with mass  $M \simeq 10^6 M_\odot$  at redshift  $z_i$ , we define a surviving time  $\tau_{\text{ds}}$  (corresponding to a final redshift  $z_f$ ) after which the halo reaches a mass  $2M$  due to merger or accretion. There will be a probability

---

<sup>3</sup>According to the numerical simulations of Ref. [54], the result of a merger between two halos with different density profiles could attain a density profile with an intermediate cusp slope. However, in Ref. [55] it was found that the final density profile would be essentially close to the cuspiest one. Here we assume the initial density cusp  $r^{-1.9}$  of the dark-star-enhanced halos gradually shallows due to the mergers with more abundant NFW halos. This gives a conservative bound of the evolutionary effect of the halo density profiles.



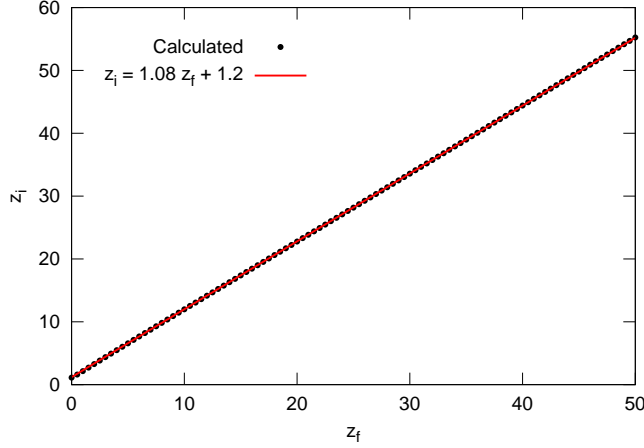


**Figure 2:** Initial redshift  $z_i$  of a halo which has a probability  $1 - 1/e$  when growing from initial mass  $M = 10^6 M_\odot$  to  $2M$  at  $z_f$ .

distribution of the final redshift  $p(z_f, 2M; z_i, M)$ . The characteristic final redshift is defined as  $P(z > z_f, 2M; z_i, M) = 1 - 1/e$ , where  $P$  is the accumulative probability that the halo reaches  $2M$  before  $z_f$ . Using the probability distribution Eq. (2.22) in Ref. [33] we find that an empirical fit  $z_i \approx 1.08z_f + 1.2$  nicely applies for the cosmological model adopted in this work, as shown in Fig. 2. As a result, the lower limit of redshift integration in Eq. (3.5) is simply taken as  $1.08z + 1.2$ . These two cases (infinite and minimum ages) bracket the possible scenarios of DS evolution history.

Replacing  $L_{\text{tot}}$  in Eq. (3.3) with  $L_{\text{tot}}^{\text{ds}}$  we can derive the enhancement factor  $\Delta_{\text{ds}}^2$  for the halos with DS formation. The enhancement factors are shown in Fig. 3. It is shown that for the most optimistic case, i.e., without LW feedback and no evolution of the DS host halos, the enhancement factor due to DM clumpiness is found to be larger by 1 – 2 orders of magnitude compared with the scenario without DS formation. However, for most other cases the additional enhancement effect due to DS formation is negligible.

### 3.3 Gamma-ray flux and constraints on DM model parameters

The  $\gamma$ -ray flux produced by DM annihilation observed today can be derived through integrating the emissivity over the evolution history of the Universe [56, 57],

$$\phi(E) = \frac{c}{4\pi} \frac{\Omega_\chi^2 \rho_c^2 \langle \sigma v \rangle}{2m_\chi^2} \int_0^\infty dz' \frac{(1+z')^3 [1 + \Delta^2(z')]}{H(z')} \frac{dN}{dE'} \exp[-\tau(z', E')], \quad (3.6)$$

where  $m_\chi$  is the mass of DM particle,  $\langle \sigma v \rangle$  is the velocity weighted annihilation cross section,  $\Omega_\chi \approx 0.23$  is the DM density parameter,  $\rho_c = 3H_0^2/8\pi G$  is the critical density of the Universe at present,  $H(z)$  is the Hubble parameter,  $E' \equiv E(1+z')$ ,  $dN/dE'$  is the  $\gamma$ -ray generation multiplicity at redshift  $z'$  for one annihilation of a pair of DM particles, and  $\tau(z', E')$  is the optical depth of the  $\gamma$ -ray photons when propagating in the intergalactic space.

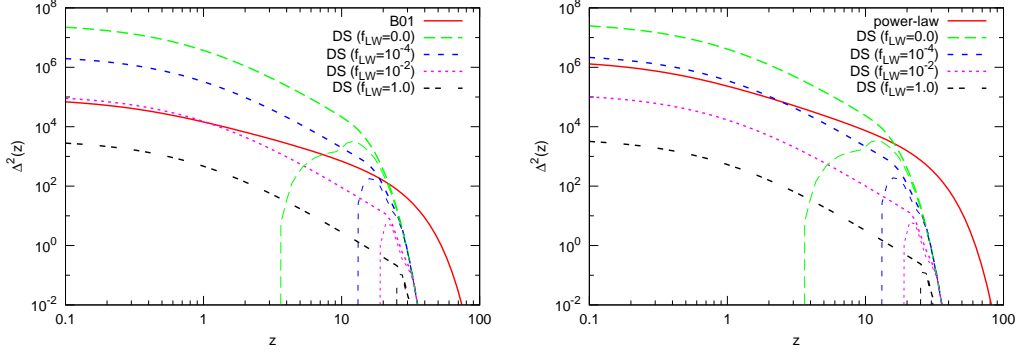


**Figure 3:** Enhancement factor of DM annihilation from clumpiness. Two concentration models, B01 (left) and power-law (right), are adopted. The red solid line is for the case without DS formation. Other lines are the enhancement factors for the halos with DS formed, for infinite (thick) and minimum (thin) age of the halos. From top to bottom the curves represent different LW efficiencies  $f_{\text{LW}} = 0.0, 10^{-4}, 10^{-2}, 1.0$  respectively.

The  $\gamma$ -ray photons of both the primary component which are generated directly from the DM annihilation products and the secondary inverse-Compton (IC) component due to scattering of DM-induced electrons/positrons off the cosmic microwave background (CMB) photons are included. The photon spectrum of the primary component for specified annihilation mode is calculated using the simulation code PYTHIA [58]. For the secondary IC component, we assume the electrons and positrons will cool instantaneously after the production [59]. Then the equilibrium  $e^\pm$  spectrum  $dn_e/dE_e$  is simply the solution of the energy loss equation

$$-\frac{\partial}{\partial E_e} \left[ \frac{dE_e}{dt} \frac{dn_e}{dE_e} \right] + \frac{dN_e}{dE_e} = 0,$$

where the energy loss rate  $dE_e/dt = 2.67 \times 10^{-17} (1+z)^4 (E_e/\text{GeV})^2 \text{ GeV s}^{-1}$ ,  $dN_e/dE_e$  is the production  $e^\pm$  multiplicity per annihilation. Then the IC photon spectrum can be calculated through convolving the  $e^\pm$  spectrum with the CMB photon spectrum and the Klein-Nishina differential cross section [60].

The processes absorbing  $\gamma$ -ray photons include photo-ionization, photon-nuclei pair production, Compton scattering, photon-photon scattering and photon-photon pair production [61, 62]. For redshift lower than 6, we also consider the pair production when scattering off the cosmic infrared background, adopting the “baseline” model in Ref. [63].

We first consider the canonical neutralino-like DM model. The expected EGRB fluxes for  $m_\chi = 100 \text{ GeV}$ ,  $\langle\sigma v\rangle = 3 \times 10^{-26} \text{ cm}^3 \text{ s}^{-1}$ ,  $b\bar{b}$  final state are shown in the upper panels of Fig. 4. The left panel is for B01 concentration model, and the right one is for power-law concentration. The solid line denotes the ordinary model without DS formation. Several DS models are plotted to show the enhancement effect of DS formation:  $f_{\text{LW}} = 0$ ,  $\tau_{\text{ds}} = \infty$  (long dashed);  $f_{\text{LW}} = 10^{-4}$ ,  $\tau_{\text{ds}} = \infty$  (short dashed);  $f_{\text{LW}} = 0$  with minimum  $\tau_{\text{ds}}$  (dotted). We can see that for the case with the strongest DS enhancement the expected EGRB will exceed the Fermi data and should be excluded. On the other hand, for the models without DS formation or models with moderate DS enhancement, the data can not give very strong

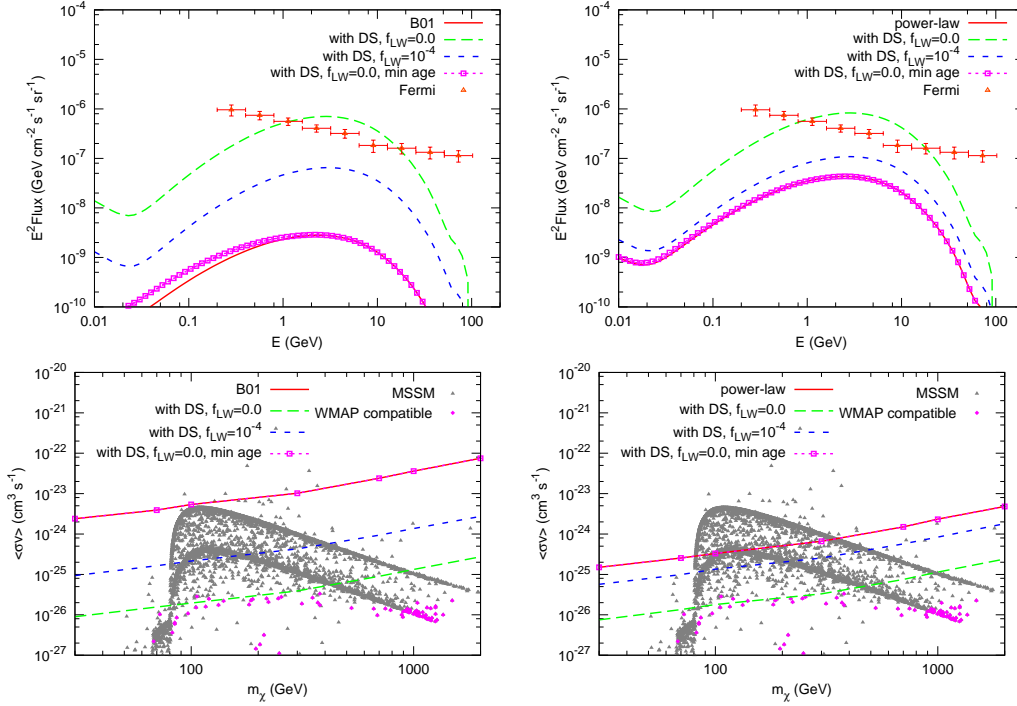


**Figure 4:** Upper panels: comparison of the expected EGRB fluxes from DM annihilation with the observational data by Fermi [18]. The particle parameters of DM are adopted as the canonical neutralino-like WIMP models with  $m_\chi = 100$  GeV,  $\langle\sigma v\rangle = 3 \times 10^{-26} \text{ cm}^3 \text{ s}^{-1}$ , and  $b\bar{b}$  annihilation final state. Lower panels: constraints on the  $m_\chi - \langle\sigma v\rangle$  parameter plane of the DM (regions below the lines are allowed). The dots show the random scan of the MSSM model parameters with DarkSUSY [64], with relic density of DM compatible with (diamond) or lower than (triangle) WMAP observational result. The left and right panels are for B01 and power-law concentrations respectively.

constraint.

The exclusion limits on the  $m_\chi - \langle\sigma v\rangle$  plane, above which the parameter space is excluded, are shown in the lower panels of Fig. 4. Here the constraints are derived by requiring that the EGRB not to exceed the  $2\sigma$  errorbars of the Fermi data, like the conservative method given in [65]. Actually since the spectral shape of Fermi data is very different from that expected from DM annihilation, we can assume a power-law background and expect to give a much stronger constraint on the DM contribution [65]. For comparison we also give the supersymmetric model predicted parameters through a random scan of the parameter space of the Minimal Supersymmetric extension of the Standard Model (MSSM), using DarkSUSY package [64]. It is shown that for the model with the largest DS enhancement, a large part of the MSSM parameter space can be excluded. The exclusion limits even reach the range required by the relic density of DM if DM is produced thermally in the early Universe.

What of most interest are the recent discoveries of the high energy electron/positron excesses by PAMELA [13], ATIC [14], HESS [15, 16] and Fermi [17]. Together with the

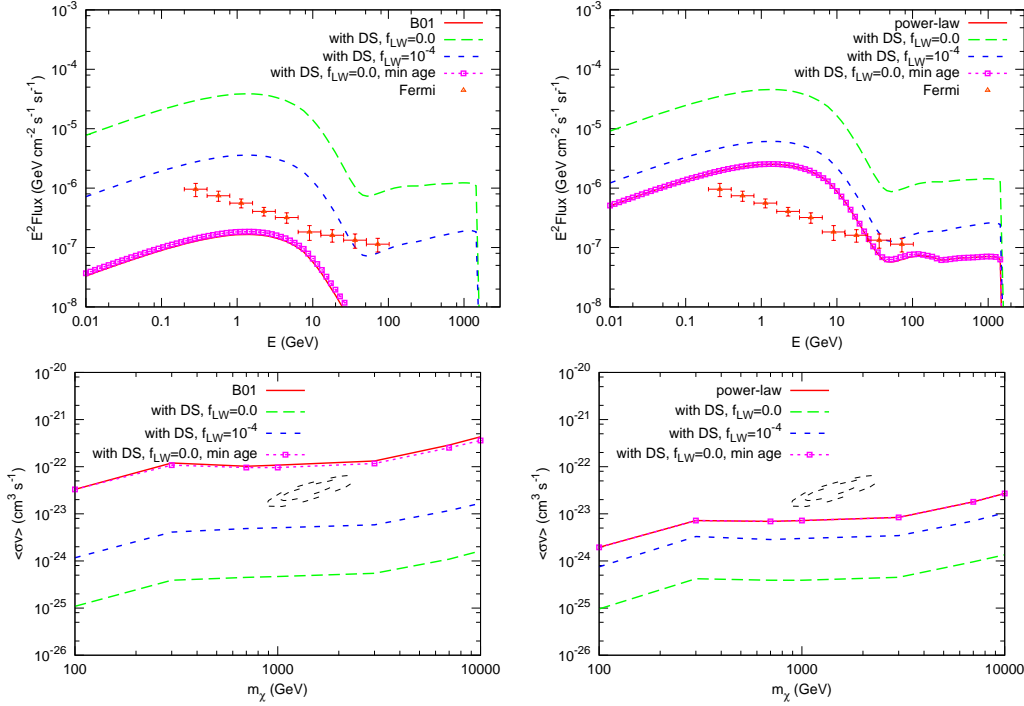


**Figure 5:** Same as Fig. 4 but for leptonic DM model with  $\mu^+\mu^-$  annihilation final state, which is proposed to be able to explain the recent observed electron/positron excesses. The mass of DM is  $m_\chi = 1.7$  TeV, and the annihilation cross section is  $\langle\sigma v\rangle = 3.6 \times 10^{-23} \text{ cm}^3 \text{ s}^{-1}$ . In the lower panels the contours are  $3\sigma$  and  $5\sigma$  confidence regions of the fit to PAMELA/Fermi/HESS electron and positron data [66].

non-excess of antiproton-proton ratio [67], the leptonic DM model is favored if DM is responsible for the excesses (e.g., [68, 69, 70, 71, 72, 73, 74, 66, 75, 76]). Alternatively, many astrophysical models have been proposed to interpret the signature (see [77] for a review). In this work we consider the DM annihilating to  $\mu^+\mu^-$  or  $\tau^+\tau^-$  final states, which are proposed to fit the PAMELA/Fermi/HESS data of positrons and electrons.

The results for  $\mu^+\mu^-$  final state are presented in Fig. 5. In the upper panels, the illustrating EGRB fluxes for  $m_\chi = 1.7$  TeV and  $\langle\sigma v\rangle = 3.6 \times 10^{-23} \text{ cm}^3 \text{ s}^{-1}$  are shown. The lower panels give the exclusion limits on the  $m_\chi - \langle\sigma v\rangle$  plane. The dashed contours in the lower panels are the  $3\sigma$  and  $5\sigma$  confidence regions of the fit to PAMELA/Fermi/HESS electron and positron data [66]. We can see that even for the case without DS enhancement, the  $e^\pm$  favored parameter regions are excluded for power-law concentration model by the Fermi EGRB data. For B01 concentration model the exclusion limit is also very close to the  $e^\pm$  favored region<sup>4</sup> (note here the exclusion limits are very conservative). If the DS enhancement is non-negligible, the constraints will be even more stringent. For the DS scenario with strong enhancement ( $f_{\text{LW}} = 0$ ,  $\tau_{\text{ds}} = \infty$ ) and moderate enhancement ( $f_{\text{LW}} = 10^{-4}$ ,  $\tau_{\text{ds}} = \infty$ ), the model explaining the  $e^\pm$  excesses can be well excluded.

<sup>4</sup>Compared with the similar semi-analytical model “BulSub” of Ref. [65], the constraint is weaker here because the subhalos inside each halo are not considered.

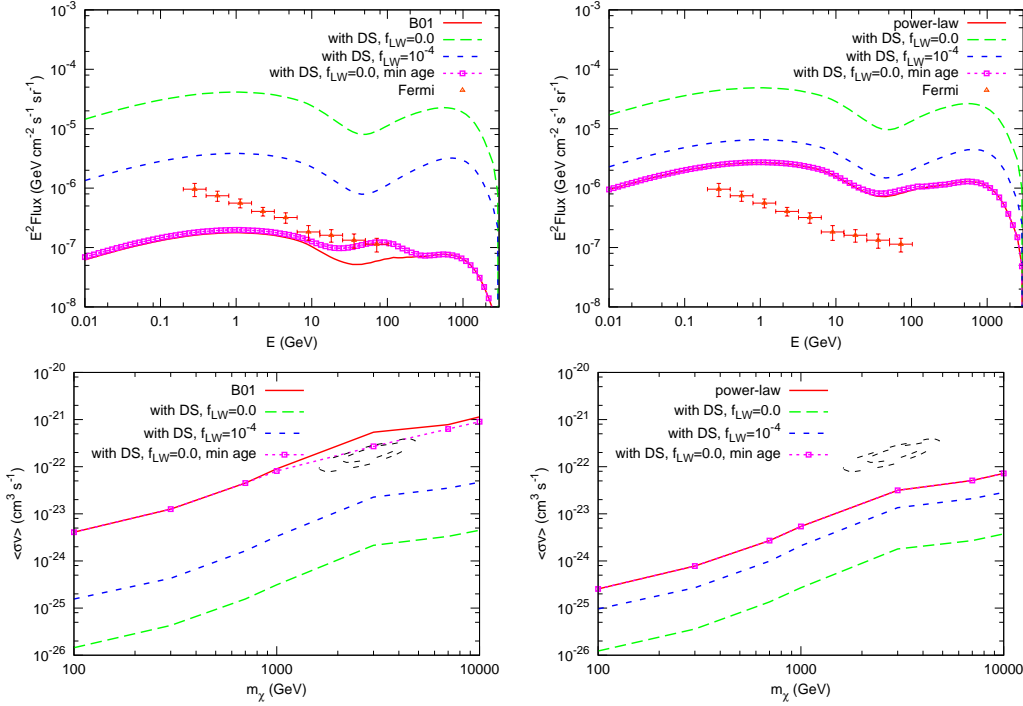


**Figure 6:** Same as Fig. 5 but for leptonic DM model with  $\tau^+\tau^-$  annihilation final state. The mass of DM is  $m_\chi = 3$  TeV, and the annihilation cross section is  $\langle\sigma v\rangle = 1.9 \times 10^{-22} \text{ cm}^3 \text{ s}^{-1}$ .

The results for  $\tau^+\tau^-$  final state are shown in Fig. 6. The DM model parameters chosen for illustration are  $m_\chi = 3$  TeV and  $\langle\sigma v\rangle = 1.9 \times 10^{-22} \text{ cm}^3 \text{ s}^{-1}$ . Similar conclusions as the  $\mu^+\mu^-$  case can be drawn.

#### 4. Conclusion and discussion

In this work we study the constraints on the DM parameters using the Fermi measured isotropic  $\gamma$ -ray data, taking into account the formation of DSs accompanied with the Pop III stars. The DS formation is expected to result in a halo with enhanced density distribution of DM, which can give larger annihilation luminosity and produce higher  $\gamma$ -ray fluxes. Two kinds of DM particle models are discussed: the canonical neutralino-like particle, and the leptonic DM which might be responsible for the  $e^\pm$  excesses.

The formation rate of DSs is closely related to the SFR of Pop III stars. We employ an analytical way to calculate the SFR of Pop III stars. The LW feedback from the Pop III stars themselves and the galaxies is considered. However, there is large uncertainty of the self-shielding effect of the LW photons. A phenomenological LW efficiency parameter  $f_{\text{LW}}$  is employed to parameterize different efficiency of the LW feedback. The results show that different  $f_{\text{LW}}$  can give very different SFR of Pop III stars, and hence the enhancement effect of DM annihilation luminosity of the DS host halos is very different. For the case with little LW feedback ( $f_{\text{LW}} \lesssim 10^{-4}$ ) the enhancement due to DS formation can be remarkable.

Another large uncertainty is the evolution effect of the DM halos once DSs were formed. The halos will be subject to mergers during the evolution of the Universe. But the change of the density profile is not clear after the major merger of two halos with different initial profiles. Some of the numerical simulations suggest that the resulting density profile will be some intermediate profile after the major merger [54], however, there are also simulations showing the final density profile will be essentially close to the cuspier one [55]. Furthermore the accretion or minor merger may also affect the evolution of the halo profile. We adopt two extreme approaches to cover the evolution effects. One is that there is no evolution of the DS host halos after their formation. The other is that the DS host halos experience a fast evolution with minimum age, which means the cuspy density profile after DS formation will disappear soon due to one major merger. These two approaches will give very different enhancement effects of the DS host halos. We hope further numerical simulations will help to clarify this issue.

There are other uncertainties such as mass function, parameters of first stars, density profile of DM halos after adiabatic contraction, fragmentation during the formation of the first stars. However, compared with the above two major uncertainties, these uncertainties are expected to be much smaller. For example, we tested that if the mass function is adopted as the PS form with  $(A, a, p) = (0.5, 1, 0)$  [23], the change of the enhancement factor is within a factor of 2.

Given these large uncertainties, especially those from the SFR and halo evolution effect, our conclusion is also model dependent. We find that in the most optimistic case for  $\gamma$ -ray production through DM annihilation, i.e., weak LW feedback and no evolution, the DS host halos would enhance the  $\gamma$ -ray signals by 1 – 2 orders of magnitude. In this case, the constraints on the cross section of the neutralino-like DM can reach the thermal production range ( $\sim 10^{-26} \text{ cm}^3 \text{ s}^{-1}$ ). The leptonic DM models proposed to explain the  $e^\pm$  excesses can be well excluded, and the excess features would be most likely of an astrophysical origin (e.g., [77]). Conversely, if the  $e^\pm$  excesses are of a DM annihilation origin, then the early Universe environment should be such that no DS can form.

In other cases with stronger LW feedback and/or minimum age of the DS host halos, the DS enhancement is much smaller and the constraints are much weaker. However, for the power-law model, due to the large contribution of many low mass halos the constraints on the models to explain  $e^\pm$  excesses still apply.

We point out that our constraints are conservative to some extent in several aspects. First, the constraints are derived according to the  $2\sigma$  upper bounds of the error bars of the data. Since the observational spectrum is essentially a single power-law shape which is very different from the DM expected spectrum, one would expect the contribution of DM component to the EGRB would be even lower than the observational data [65]. Using that reduced background would give more stringent constraints on the DS formation scenarios and DM annihilation model. Furthermore, there are sub-halos and sub-sub-halos in each halo, which may give even stronger annihilation signals [78]. Considering this effect would pose even stringent constraints. Finally, only the adiabatic contraction processes accompanied with the first star formation are included. There should be many other adiabatic contraction processes, e.g. during the formation of the second and third generation stars,

which should also give enhanced DM distribution.

## Acknowledgments

We thank Kentaro Nagamine for helpful discussion on dark matter halo evolution in the early Universe and the comments on the draft. QY thanks Ann Zabludoff for discussion on the impact of dark star on the first star formation rate. This work is supported by NSF under grant AST-0908362, NASA under grants NNX10AP53G and NNX10AD48G, and Natural Sciences Foundation of China under grant 11073024, and the 973 project under grant 2007CB815401.

## References

- [1] D. Spolyar, K. Freese, and P. Gondolo, *Dark Matter and the First Stars: A New Phase of Stellar Evolution*, *Physical Review Letters* **100** (Feb., 2008) 051101, [[arXiv:0705.0521](#)].
- [2] F. Iocco, *Dark Matter Capture and Annihilation on the First Stars: Preliminary Estimates*, *Astrophys. J. Lett.* **677** (Apr., 2008) L1–L4, [[arXiv:0802.0941](#)].
- [3] K. Freese, P. Bodenheimer, D. Spolyar, and P. Gondolo, *Stellar Structure of Dark Stars: A First Phase of Stellar Evolution Resulting from Dark Matter Annihilation*, *Astrophys. J. Lett.* **685** (Oct., 2008) L101–L104, [[arXiv:0806.0617](#)].
- [4] K. Freese, D. Spolyar, and A. Aguirre, *Dark matter capture in the first stars: a power source and limit on stellar mass*, *J. Cosmol. Astropart. Phys.* **11** (Nov., 2008) 14–+, [[arXiv:0802.1724](#)].
- [5] F. Iocco, A. Bressan, E. Ripamonti, R. Schneider, A. Ferrara, and P. Marigo, *Dark matter annihilation effects on the first stars*, *Mon. Not. Roy. Astron. Soc.* **390** (Nov., 2008) 1655–1669, [[arXiv:0805.4016](#)].
- [6] M. Taoso, G. Bertone, G. Meynet, and S. Ekström, *Dark matter annihilations in Population III stars*, *Phys. Rev. D* **78** (Dec., 2008) 123510–+, [[arXiv:0806.2681](#)].
- [7] A. Natarajan, J. C. Tan, and B. W. O’Shea, *Dark Matter Annihilation and Primordial Star Formation*, *Astrophys. J.* **692** (Feb., 2009) 574–583, [[arXiv:0807.3769](#)].
- [8] D. Spolyar, P. Bodenheimer, K. Freese, and P. Gondolo, *Dark Stars: A New Look at the First Stars in the Universe*, *Astrophys. J.* **705** (Nov., 2009) 1031–1042, [[arXiv:0903.3070](#)].
- [9] K. Freese, C. Ilie, D. Spolyar, M. Valluri, and P. Bodenheimer, *Supermassive Dark Stars: Detectable in JWST*, *Astrophys. J.* **716** (June, 2010) 1397–1407, [[arXiv:1002.2233](#)].
- [10] E. Zackrisson, P. Scott, C. Rydberg, F. Iocco, B. Edvardsson, G. Östlin, S. Sivertsson, A. Zitrin, T. Broadhurst, and P. Gondolo, *Finding High-redshift Dark Stars with the James Webb Space Telescope*, *Astrophys. J.* **717** (July, 2010) 257–267, [[arXiv:1002.3368](#)].
- [11] D. R. G. Schleicher, R. Banerjee, and R. S. Klessen, *Dark stars: Implications and constraints from cosmic reionization and extragalactic background radiation*, *Phys. Rev. D* **79** (Feb., 2009) 043510, [[arXiv:0809.1519](#)].
- [12] P. Sandick, J. Diemand, K. Freese and D. Spolyar, *Black holes in our galactic halo: compatibility with FGST and PAMELA data and constraints on the first stars background radiation*, *J. Cosmol. Astropart. Phys.* **01** (Jan., 2011) 018, [[arXiv:1008.3552](#)].

- [13] O. Adriani *et al.*, *An anomalous positron abundance in cosmic rays with energies 1.5-100 GeV*, *Nature* **458** (Apr., 2009) 607–609, [arXiv:0810.4995].
- [14] J. Chang *et al.*, *An excess of cosmic ray electrons at energies of 300-800 GeV*, *Nature* **456** (Nov., 2008) 362–365.
- [15] F. Aharonian *et al.*, *Energy Spectrum of Cosmic-Ray Electrons at TeV Energies*, *Phys. Rev. Lett.* **101** (Dec., 2008) 261104, [arXiv:0811.3894].
- [16] F. Aharonian *et al.*, *Probing the ATIC peak in the cosmic-ray electron spectrum with H.E.S.S.*, *Astron. Astrophys.* **508** (Dec., 2009) 561–564.
- [17] A. A. Abdo *et al.*, *Measurement of the Cosmic Ray  $e^+ + e^-$  Spectrum from 20 GeV to 1 TeV with the Fermi Large Area Telescope*, *Phys. Rev. Lett.* **102** (May, 2009) 181101, [arXiv:0905.0025].
- [18] A. A. Abdo *et al.*, *Spectrum of the Isotropic Diffuse Gamma-Ray Emission Derived from First-Year Fermi Large Area Telescope Data*, *Physical Review Letters* **104** (Mar., 2010) 101101.
- [19] P. Sreekumar *et al.*, *EGRET Observations of the Extragalactic Gamma-Ray Emission*, *Astrophys. J.* **494** (Feb., 1998) 523, [astro-ph/].
- [20] E. Komatsu *et al.*, *Five-Year Wilkinson Microwave Anisotropy Probe Observations: Cosmological Interpretation*, *Astrophys. J. Supp.* **180** (Feb., 2009) 330–376, [arXiv:0803.0547].
- [21] E. Komatsu *et al.*, *Seven-year Wilkinson Microwave Anisotropy Probe (WMAP) Observations: Cosmological Interpretation*, *Astrophys. J. Supp.* **192** (Feb., 2011) 18–+, [arXiv:1001.4538].
- [22] S. M. Carroll, W. H. Press, and E. L. Turner, *The cosmological constant*, *Annu. Rev. Astron. Astrophys.* **30** (1992) 499–542.
- [23] W. H. Press and P. Schechter, *Formation of Galaxies and Clusters of Galaxies by Self-Similar Gravitational Condensation*, *Astrophys. J.* **187** (Feb., 1974) 425–438.
- [24] R. K. Sheth and G. Tormen, *Large-scale bias and the peak background split*, *Mon. Not. Roy. Astron. Soc.* **308** (Sept., 1999) 119–126, [astro-ph/].
- [25] J. M. Bardeen, J. R. Bond, N. Kaiser, and A. S. Szalay, *The statistics of peaks of Gaussian random fields*, *Astrophys. J.* **304** (May, 1986) 15–61.
- [26] X. Chen and J. Miralda-Escudé, *The 21 cm Signature of the First Stars*, *Astrophys. J.* **684** (Sept., 2008) 18–33, [astro-ph/].
- [27] M. Trenti and M. Stiavelli, *Formation Rates of Population III Stars and Chemical Enrichment of Halos during the Reionization Era*, *Astrophys. J.* **694** (Apr., 2009) 879–892, [arXiv:0901.0711].
- [28] M. J. Turk, T. Abel, and B. O’Shea, *The Formation of Population III Binaries from Cosmological Initial Conditions*, *Science* **325** (July, 2009) 601–, [arXiv:0907.2919].
- [29] D. Schaerer, *On the properties of massive Population III stars and metal-free stellar populations*, *Astron. Astrophys.* **382** (Jan., 2002) 28–42, [astro-ph/].
- [30] U. Maio, B. Ciardi, K. Dolag, L. Tornatore, and S. Khochfar, *The transition from population III to population II-I star formation*, *Mon. Not. Roy. Astron. Soc.* **407** (Sept., 2010) 1003–1015, [arXiv:1003.4992].



- [31] S. Sivertsson and P. Gondolo, *The WIMP capture process for dark stars in the early universe*, *ArXiv e-prints:1006.0025* (May, 2010) [[arXiv:1006.0025](#)].
- [32] E. Ripamonti, F. Iocco, A. Ferrara, R. Schneider, A. Bressan, and P. Marigo, *First star formation with dark matter annihilation*, *Mon. Not. Roy. Astron. Soc.* **406** (Aug., 2010) 2605–2615, [[arXiv:1003.0676](#)].
- [33] C. Lacey and S. Cole, *Merger rates in hierarchical models of galaxy formation*, *Mon. Not. Roy. Astron. Soc.* **262** (June, 1993) 627–649.
- [34] A. Heger and S. E. Woosley, *The Nucleosynthetic Signature of Population III*, *Astrophys. J.* **567** (Mar., 2002) 532–543, [[astro-ph/](#)].
- [35] T. H. Greif and V. Bromm, *Two populations of metal-free stars in the early Universe*, *Mon. Not. Roy. Astron. Soc.* **373** (Nov., 2006) 128–138, [[astro-ph/](#)].
- [36] D. Schaerer, *The transition from Population III to normal galaxies: Ly $\alpha$  and He II emission and the ionising properties of high redshift starburst galaxies*, *Astron. Astrophys.* **397** (Jan., 2003) 527–538, [[astro-ph/](#)].
- [37] G. Mellema, I. T. Iliev, U. Pen, and P. R. Shapiro, *Simulating cosmic reionization at large scales - II. The 21-cm emission features and statistical signals*, *Mon. Not. Roy. Astron. Soc.* **372** (Oct., 2006) 679–692, [[astro-ph/](#)].
- [38] D. A. Verner and G. J. Ferland, *Atomic Data for Astrophysics. I. Radiative Recombination Rates for H-like, He-like, Li-like, and Na-like Ions over a Broad Range of Temperature*, *Astrophys. J. Supp.* **103** (Apr., 1996) 467–+, [[astro-ph/](#)].
- [39] N. Yoshida, T. Abel, L. Hernquist, and N. Sugiyama, *Simulations of Early Structure Formation: Primordial Gas Clouds*, *Astrophys. J.* **592** (Aug., 2003) 645–663, [[astro-ph/](#)].
- [40] A. M. Hopkins and J. F. Beacom, *On the Normalization of the Cosmic Star Formation History*, *Astrophys. J.* **651** (Nov., 2006) 142–154, [[astro-ph/](#)].
- [41] M. Kawasaki, K. Kohri, and K. Nakayama, *Diffuse gamma-ray background and cosmic-ray positrons from annihilating dark matter*, *Phys. Rev. D* **80** (July, 2009) 023517, [[arXiv:0904.3626](#)].
- [42] Q. Yuan, B. Yue, X. Bi, X. Chen, and X. Zhang, *Leptonic dark matter annihilation in the evolving universe: constraints and implications*, *J. Cosmol. Astropart. Phys.* **10** (Oct., 2010) 23–+, [[arXiv:0912.2504](#)].
- [43] J. F. Navarro, C. S. Frenk, and S. D. M. White, *A Universal Density Profile from Hierarchical Clustering*, *Astrophys. J.* **490** (Dec., 1997) 493, [[astro-ph/](#)].
- [44] B. Moore, T. Quinn, F. Governato, J. Stadel, and G. Lake, *Cold collapse and the core catastrophe*, *Mon. Not. Roy. Astron. Soc.* **310** (Dec., 1999) 1147–1152, [[astro-ph/](#)].
- [45] Y. P. Jing and Y. Suto, *The Density Profiles of the Dark Matter Halo Are Not Universal*, *Astrophys. J. Lett.* **529** (Feb., 2000) L69–L72, [[astro-ph/](#)].
- [46] J. F. Navarro *et al.*, *The inner structure of  $\Lambda$ CDM haloes - III. Universality and asymptotic slopes*, *Mon. Not. Roy. Astron. Soc.* **349** (Apr., 2004) 1039–1051, [[astro-ph/](#)].
- [47] J. F. Navarro *et al.*, *The diversity and similarity of simulated cold dark matter haloes*, *Mon. Not. Roy. Astron. Soc.* **402** (Feb., 2010) 21–34, [[arXiv:0810.1522](#)].

- [48] A. W. Graham, D. Merritt, B. Moore, J. Diemand and B. Terzic, *Empirical Models for Dark Matter Halos. II. Inner Profile Slopes, Dynamical Profiles, and  $\rho/\sigma^3$* , *Astron. J.* **132** (Dec., 2006) 2701–2710 [[arXiv:astro-ph/0608613](#)].
- [49] J. S. Bullock *et al.*, *Profiles of dark haloes: evolution, scatter and environment*, *Mon. Not. Roy. Astron. Soc.* **321** (Mar., 2001) 559–575, [[astro-ph/](#)].
- [50] A. V. Macciò, A. A. Dutton, and F. C. van den Bosch, *Concentration, spin and shape of dark matter haloes as a function of the cosmological model: WMAP1, WMAP3 and WMAP5 results*, *Mon. Not. Roy. Astron. Soc.* **391** (Dec., 2008) 1940–1954, [[arXiv:0805.1926](#)].
- [51] D. H. Zhao, Y. P. Jing, H. J. Mo, and G. Börner, *Accurate Universal Models for the Mass Accretion Histories and Concentrations of Dark Matter Halos*, *Astrophys. J.* **707** (Dec., 2009) 354–369, [[arXiv:0811.0828](#)].
- [52] A. Klypin, S. Trujillo-Gomez, and J. Primack, *Halos and galaxies in the standard cosmological model: results from the Bolshoi simulation*, *ArXiv e-prints:1002.3660* (Feb., 2010) [[arXiv:1002.3660](#)].
- [53] K. Freese, P. Gondolo, J. A. Sellwood, and D. Spolyar, *Dark Matter Densities During the Formation of the First Stars and in Dark Stars*, *Astrophys. J.* **693** (Mar., 2009) 1563–1569, [[arXiv:0805.3540](#)].
- [54] M. Boylan-Kolchin and C.-P. Ma, *Major mergers of galaxy haloes: cuspy or cored inner density profile?*, *Mon. Not. Roy. Astron. Soc.* **349** (Apr., 2004) 1117–1129, [[astro-ph/](#)].
- [55] S. Kazantzidis, A. R. Zentner, and A. V. Kravtsov, *The Robustness of Dark Matter Density Profiles in Dissipationless Mergers*, *Astrophys. J.* **641** (Apr., 2006) 647–664, [[astro-ph/](#)].
- [56] P. Ullio, L. Bergström, J. Edsjö, and C. Lacey, *Cosmological dark matter annihilations into  $\gamma$  rays: A closer look*, *Phys. Rev. D* **66** (Dec., 2002) 123502, [[astro-ph/](#)].
- [57] G. Hütsi, A. Hektor, and M. Raidal, *Constraints on leptonically annihilating dark matter from reionization and extragalactic gamma background*, *Astron. Astrophys.* **505** (Oct., 2009) 999–1005, [[arXiv:0906.4550](#)].
- [58] T. Sjöstrand, S. Mrenna, and P. Skands, *PYTHIA 6.4 physics and manual*, *Journal of High Energy Physics* **5** (May, 2006) 26, [[hep-ph/06](#)].
- [59] S. Profumo and T. E. Jeltema, *Extragalactic Inverse Compton Light from Dark Matter annihilation and the Pamela positron excess*, *Journal of Cosmology and Astro-Particle Physics* **7** (July, 2009) 20, [[arXiv:0906.0001](#)].
- [60] G. R. Blumenthal and R. J. Gould, *Bremsstrahlung, Synchrotron Radiation, and Compton Scattering of High-Energy Electrons Traversing Dilute Gases*, *Reviews of Modern Physics* **42** (1970) 237–271.
- [61] A. A. Zdziarski and R. Svensson, *Absorption of X-rays and gamma rays at cosmological distances*, *Astrophys. J.* **344** (Sept., 1989) 551–566.
- [62] X. Chen and M. Kamionkowski, *Particle decays during the cosmic dark ages*, *Phys. Rev. D* **70** (Aug., 2004) 043502, [[astro-ph/](#)].
- [63] F. W. Stecker, M. A. Malkan, and S. T. Scully, *Intergalactic Photon Spectra from the Far-IR to the UV Lyman Limit for  $0 < z < 6$  and the Optical Depth of the Universe to High-Energy Gamma Rays*, *Astrophys. J.* **648** (Sept., 2006) 774–783, [[astro-ph/](#)].

- [64] P. Gondolo, J. Edsjö, P. Ullio, L. Bergström, M. Schelke, and E. A. Baltz, *DarkSUSY: computing supersymmetric dark matter properties numerically*, *Journal of Cosmology and Astro-Particle Physics* **7** (July, 2004) 8, [[astro-ph/](#)].
- [65] A. A. Abdo *et al.*, *Constraints on cosmological dark matter annihilation from the Fermi-LAT isotropic diffuse gamma-ray measurement*, *Journal of Cosmology and Astro-Particle Physics* **4** (Apr., 2010) 14.
- [66] P. Meade, M. Papucci, A. Strumia, and T. Volansky, *Dark Matter interpretations of the  $e^\pm$  excesses after FERMI*, *Nuclear Physics B* **831** (May, 2010) 178–203, [[arXiv:0905.0480](#)].
- [67] O. Adriani *et al.*, *New Measurement of the Antiproton-to-Proton Flux Ratio up to 100 GeV in the Cosmic Radiation*, *Phys. Rev. Lett.* **102** (Feb., 2009) 051101, [[arXiv:0810.4994](#)].
- [68] L. Bergström, T. Bringmann, and J. Edsjö, *New positron spectral features from supersymmetric dark matter: A way to explain the PAMELA data?*, *Phys. Rev. D* **78** (Nov., 2008) 103520, [[arXiv:0808.3725](#)].
- [69] M. Cirelli, M. Kadastik, M. Raidal, and A. Strumia, *Model-independent implications of the  $e^\pm$ ,  $\bar{p}$  cosmic ray spectra on properties of Dark Matter*, *Nuclear Physics B* **813** (May, 2009) 1–21, [[arXiv:0809.2409](#)].
- [70] P. F. Yin, Q. Yuan, J. Liu, J. Zhang, X. J. Bi, S. H. Zhu, and X. M. Zhang, *PAMELA data and leptonically decaying dark matter*, *Phys. Rev. D* **79** (Jan., 2009) 023512, [[arXiv:0811.0176](#)].
- [71] I. Cholis, G. Dobler, D. P. Finkbeiner, L. Goodenough, and N. Weiner, *Case for a 700+GeV WIMP: Cosmic ray spectra from PAMELA, Fermi, and ATIC*, *Phys. Rev. D* **80** (Dec., 2009) 123518, [[arXiv:0811.3641](#)].
- [72] N. Arkani-Hamed, D. P. Finkbeiner, T. R. Slatyer, and N. Weiner, *A theory of dark matter*, *Phys. Rev. D* **79** (Jan., 2009) 015014, [[arXiv:0810.0713](#)].
- [73] L. Bergström, J. Edsjö, and G. Zaharijas, *Dark Matter Interpretation of Recent Electron and Positron Data*, *Physical Review Letters* **103** (July, 2009) 031103, [[arXiv:0905.0333](#)].
- [74] D. Hooper and K. M. Zurek, *PAMELA, FGST and sub-TeV dark matter*, *Physics Letters B* **691** (July, 2010) 18–31, [[arXiv:0909.4163](#)].
- [75] C. Pallis, *Cold dark matter in non-standard cosmologies, PAMELA, ATIC and Fermi LAT*, *Nuclear Physics B* **831** (May, 2010) 217–247, [[arXiv:0909.3026](#)].
- [76] K. Ishiwata, S. Matsumoto, and T. Moroi, *Decaying dark matter in supersymmetric model and cosmic-ray observations*, *Journal of High Energy Physics* **12** (Dec., 2010) 6–+, [[arXiv:1008.3636](#)].
- [77] Y.-Z. Fan, B. Zhang, and J. Chang, *Electron/positron Excesses in the Cosmic Ray Spectrum and Possible Interpretations*, *International Journal of Modern Physics D* **19** (2010) 2011–2058, [[arXiv:1008.4646](#)].
- [78] J. Zavala, V. Springel, and M. Boylan-Kolchin, *Extragalactic gamma-ray background radiation from dark matter annihilation*, *Mon. Not. Roy. Astron. Soc.* **405** (Jun., 2010) 593–612, [[arXiv:0908.2428](#)].